

# Optical properties of $\text{Al}_2\text{O}_3/\text{Al}$ cermets obtained by plasma spraying: role of composition and microstructure

D. Toru<sup>1</sup>, K. Wittmann-Ténèze<sup>1</sup>, A. Quet<sup>1</sup>, D. Damiani<sup>1</sup>, H. Piombini<sup>1</sup>,  
D. De Sousa Meneses<sup>2</sup>, L. Del Campo<sup>2</sup> and P. Echegut<sup>2</sup>

<sup>1</sup> CEA Le Ripault  
BP 16, 37 260 Monts, France

<sup>2</sup> CEMHTI  
1 avenue de la Recherche Scientifique, 45 100 Orleans, France

**Abstract**  $\text{Al}_2\text{O}_3/\text{Al}$  cermets (ceramic/metal) have been made by plasma spraying with different metal concentration in order to study their optical properties. A metal has a high reflectivity in the visible and the IR region, but the optical behaviour of an oxide ceramic is much more complicated, mainly if synthesised by plasma spraying. Indeed, a crystallised and dense ceramic, as alumina for example, is widely transparent in the visible region up to  $5\ \mu\text{m}$ , whereas in the same range of wavelength a ceramic synthesised by thermal spray will be broadly reflective. Due to its specific microstructure, plasma sprayed coatings include intrinsic open and closed porosity (5 to 20%), rough surfaces and a lamellar microstructure. Plasma operating parameters have been selected during a preliminary study of pure alumina: the nature of the plasma gas, the spray distance, and the powder feed rate. Same parameters were used to realise cermet coatings, with a double injection system. Optical properties of as-sprayed and polished coatings are discussed. The reflectance rises with the aluminium concentration, but in the transparent region of alumina ( $1 < \lambda < 5\ \mu\text{m}$ ), we notice a remarkable behaviour for low aluminium concentration where the reflectance of a cermet is lower than pure alumina.

## 1 Introduction

Atmospheric plasma spraying (APS) is a process in which particles are deposited on a substrate in a molten or semi-molten state. Particles are heated in the plasma jet at very high temperature (10 000 to 15 000 K), and propelled at high velocity to impact the substrate where they flatten and rapidly solidify [1]. The great advantage of this process is its ability to spray a wide range of materials, from metals to ceramics, on a large variety of geometries and sizes of substrates. In addition, it is an inexpensive technique which enables to produce thick coatings with thicknesses ranging from 50  $\mu\text{m}$  to few millimetres. Plasma sprayed coatings confer industrial solutions for heat and oxidation protection, wear and erosion resistance, high temperature applications, but few studies were carried on optical properties [2–5].

Conventional plasma sprayed coatings have a lamellar and heterogeneous microstructure, include a multi-scaled open and closed porosity (5 to 20%), and have rough surfaces. As a consequence, optical properties of plasma sprayed coatings are different compared to ones known for homogeneous materials obtained by thin film processes as PVD or sol-gel. For homogeneous materials, the knowledge of the optical complex index and the thickness are sufficient to predict the optical behaviour. The real part of the index corresponds to the ratio between the celerity of the light in the vacuum over the celerity in the material. The imaginary part corresponds to the absorption coefficient and represents the attenuation of the radiation in the material. Then Fresnel equation and Beer law enable respectively the access to the normal reflectance and the transmittance. When light proceeds from one medium into a homogeneous solid medium, a part of the radiation can be transmitted, a part can be absorbed and the other part can be reflected at the interface between the two media. The sum of the fractions of incident light that are transmitted, absorbed and reflected is equal to unity. For heterogeneous coatings, parameters such as roughness and porosity have an influence on scattering radiation. So the optical properties depend on the complex refractive index and the microstructure of the material. Studies on the optical behaviour of porous materials showed that the reflectivity is not only linked to the optical index, but also to the type of heterogeneities in the material such as porosity, roughness, grain boundaries... [4–8]. Actually, optical properties are mainly affected by

the roughness and the porosity and grain boundary effects can be neglected [7].

In this study, the optical behaviour of plasma sprayed cermets (ceramic–metal materials) was investigated. Cermet materials possess the advantages of both ceramics and metals. By varying the amount of each material, cermets can be designed to obtain desired mechanical properties, thermal or electrical conductivity. In the same way, reflectivity and so emissivity could be adjusted through the use of cermet coatings. Low and high-emissivity coatings are of great interest in applications such as solar collectors, automotive or aeronautical components and a better understanding of the optical properties of plasma sprayed coatings would allow disposing alternative solutions in these fields. Here, aluminium and alumina were selected due to their well known optical properties. Aluminium is one of the best reflective metals. Ceramics such as alumina manufactured with a process like plasma spraying contain heterogeneities giving an optical behaviour different from a monocrystal. By modifying the metallic charge in the cermet, the evolution of the reflectance was studied for as-sprayed and polished coatings.

## 2 Experimental

### 2.1 Material

Commercially available powders were used as the starting materials: aluminium powder (Medicoat, 45-75 µm, Amperit 740.1) and alumina powder (Metco, 22-45 µm, 54NS-1). Aluminium plates with nominal dimensions of 50 x 50 x 2 mm<sup>3</sup> were used as substrates. Prior to spraying, the surface of the substrates was grit-blasted and degreased by heating. Plasma spraying was performed with a F4VB torch (Sulzer Metco) working under atmospheric pressure. Metallic and ceramic powders were fed radially and separately into the plasma jet using argon as carrier gas then heated and accelerated by the plasma jet towards the substrate. Metal was injected farther than the ceramic into the plasma jet because of the different thermal properties such as the melting point (Figure 4.1). In flight particle velocity and temperature were measured with a DPV2000 diagnostic system (Tecnar Automation, Qc, Canada). Plasma spraying makes intrinsically porous coatings. In order to minimise the impact of the porosity on optical properties, several conditions

were tested to have the densest alumina coating as possible, by varying particle velocity (200-300 m.s<sup>-1</sup>) and temperature (2300-2600 K). Studied parameters were the spray distance, the current intensity, and the composition of the plasma gas. Selected parameters are given in Table 4.1. Mixtures of *Ar – He – H<sub>2</sub>* were used as plasma gas. Cermet coatings were realized with the same set of conditions. The amount of metal was adjusted ranging from 0%<sub>wt</sub> to 100%<sub>wt</sub>.

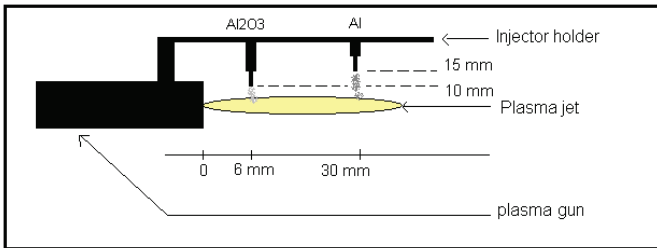


**Figure 4.1:** Schema of the double injection system.

Spray parameters for plasma spraying

Arc current intensity, A	500
Argon flow rate (%)	30
Helium flow rate (%)	54
Hydrogen flow rate (%)	16
Injector diameter, mm	1.5
Spray distance, mm	140
Powder deviation angle, °	3.5

**Table 4.1:**

## 2.2 Characterisations

Coating cross sections were observed by Scanning Electron Microscopy (SEM, LEO 440). The crystalline structure was assessed with a D5000 X-Ray Diffractometer (XRD, Siemens A.G.) using Cu K $\alpha$  radiation. Total reflectance and transmittance were measured between 1 and 20  $\mu\text{m}$  with a Bruker IFS66 spectrometer. A 7.6-mm diameter integrating sphere

with gold inner coating was used in order to collect hemispherical radiation. The porosity was estimated by Archimedean method. The roughness was measured with a Perthometer S2.

### 3 Results and discussion

The coatings were deposited up to around a 400  $\mu m$  thickness. Open porosity measured by Archimedean method was about 10%. The roughness of the as-sprayed coatings was ranged between 5 and 10  $\mu m$  because of the difference in starting particle size distribution. Surface morphology of the as-sprayed coatings is revealed in Figure 4.2(b). The roughness of the polished coatings was lower than 1  $\mu m$ . XRD analysis showed both  $\alpha$  and  $\gamma - Al_2O_3$  phases in the coatings. Optical properties are discussed through the reflectivity values obtained for three wavelengths selected according to the specific optical behaviour of alumina (2, 8 and 12  $\mu m$ ).

#### 3.1 As-sprayed single material coatings

Traditional characteristics of plasma sprayed coatings were identified [9], as the lamellar microstructure, unmelted particles and globular, interlamellar or intralamellar porosity (Figure 4.2(a)). The coatings resulted from spreading and solidification of liquid  $Al_2O_3$  droplets on the substrate. Stacking defects of lamellae can be due to unmelted particles or to imperfect spreading, inducing globular pores and interlamellar flat pores along the splats which are perpendicular to the spraying direction. Intralamellar cracks occur especially in brittle ceramic due to rapid solidification. Thus porosity made of pores and cracks of various shapes and sizes, from hundred nanometres to about ten micrometers makes complicated its characterisation and its correlation to the optical behaviour. As regards to the optical properties of the alumina coating, a part of transparency of about 25% was measured for  $1 < \lambda < 5$   $\mu m$  linked to the 400- $\mu m$  coating thickness and to the semi-transparent behavior of each alumina lamella (Figure 4.5). The first focused wavelength was 2  $\mu m$ , because it matches with this semi-transparent region [8] and highlights volume phenomena. At this wavelength, phonon vibration or water absorption peak are not present, and alumina does

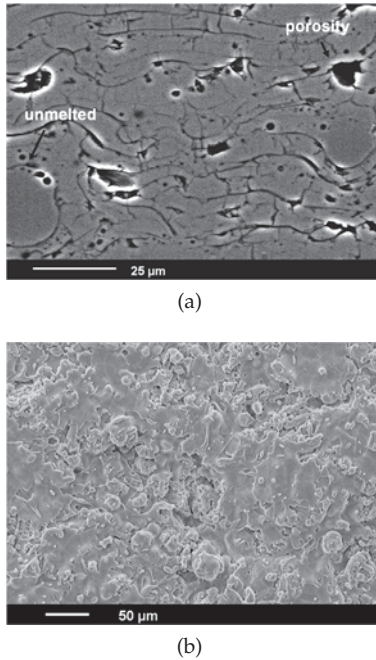


**Figure 4.2:** SEM of the  $Al_2O_3$  coating: (a) polished cross section, (b) as-sprayed surface morphology.

not absorb radiation. Despite its semi-transparent behaviour, the reflectance of the alumina coating at  $2\ \mu\text{m}$  is very high (about 80%) because of the interactions between the electromagnetic radiation and the matter. Heterogeneities induce scattering phenomena including three types of interactions [4]: (i) diffraction which results in a modified direction of light propagation around the heterogeneity; (ii) refraction which involves penetration of light in the heterogeneity, and modification of the emerging direction; and (iii) multiple reflections at the interface between the heterogeneity and the matrix medium. These interactions between radiation and alumina matrix are summarised under the term “volume scattering” in Figure 4.6. The second wavelength chosen was  $8\ \mu\text{m}$  which is near to the Christiansen wavelength and characteristic

of the opaque and the absorbent domain of the alumina comprised between 5 and 10  $\mu\text{m}$ . As a result, the reflectance is close to zero. The last selected wavelength was 12  $\mu\text{m}$ , because it matches with a domain where alumina does not only absorb but also reflects the radiation ( $10 < \lambda < 16 \mu\text{m}$ ). A monocrystal of alumina reflects about 80% of the radiation at 12  $\mu\text{m}$ , whereas a plasma sprayed coating reflects 20% due to its microstructure. At 12  $\mu\text{m}$ , the imaginary part of the alumina optical index is strong, and because the 6- $\mu\text{m}$  measured roughness was high, a large part of the radiation is absorbed due to the trapping of photons on heterogeneities.

Aluminium coatings appeared more porous than alumina; the open void content was 15%. Unmelted particles and voids are shown in Figure 4.3. As expected, the reflectance of the aluminium coating was constant and high, above 80%, for the three wavelengths (Figure 4.5). The measured roughness (about 10  $\mu\text{m}$ ) can explain that the reflectivity is lower than one obtained for an homogeneous metal. Surface scattering inducing absorption occurs.

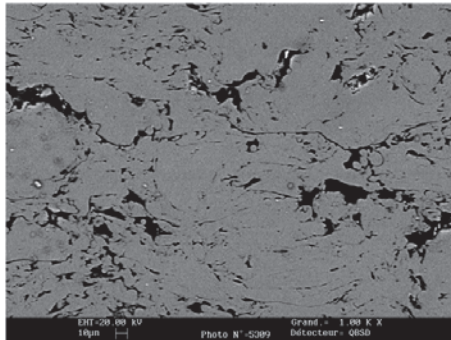
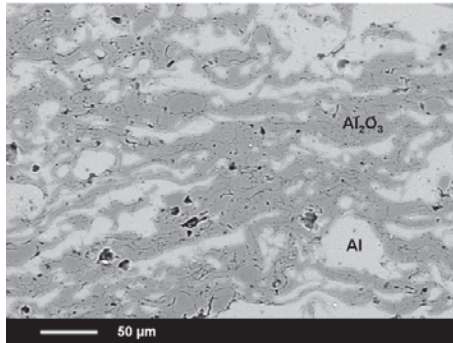


Figure 4.3: SEM polished cross section of the Al coating.

### 3.2 As-sprayed cermet coatings

For cermet coatings no transmittance was revealed from visible to IR region. Figure 4.4 shows that aluminium was homogeneously spread out, but splats present various shapes resulting from different spread-



**Figure 4.4:** SEM polished cross section of a cermet coating with 33%<sub>wt</sub> Al.

ing degree. At 2  $\mu\text{m}$ , for a low amount of aluminium in the cermet, the reflectance decreased compared with pure alumina. Mechanisms occurring in the low Al content cermets are proposed schematically in Figure 4.6. Aluminium lamellae do not only reflect a part of the existing radiation, extending therefore the path travelled by the photons in the material, but also absorb a small part of the radiation in the volume. Thus, reflectance linked to scattering effects and to alumina coating heterogeneities is softened. In addition, there are not enough metallic lamellae in the top of the coating to increase the reflectance by specular reflexion or surface scattering. Volume effects prevail on surface effects. When the metal amount is higher than 75%, the surface contribution of the metal is prevailing, so the reflectance increases compared with pure alumina (Figure 4.5). At 8  $\mu\text{m}$ , both of the materials are opaque. Close to the Christiansen wavelength, alumina is absorbent, so the reflectance level is close to zero. In this domain, only surface effects are present; no photons can penetrate into the volume. As a result, the reflectance is directly linked to the amount of aluminium in the surface: higher the aluminium quantity is, higher the reflected radiation. The same trend is observed at 12  $\mu\text{m}$ , where pure alumina is opaque as well. An additional contribution of alumina should raise the cermet reflectance values. However the reflectance appeared lower at 12  $\mu\text{m}$  than at 8  $\mu\text{m}$  independently of the metal amount. The part of the scattered reflectance

was measured and represented by dotted lines for each wavelength in Figure 4.5. It appeared that scattering contributes to the main part of the reflectance. The specular part corresponds to about 20 % of the total reflectance. These values are easily correlated to the coating roughness in the opaque region (8 and 12  $\mu\text{m}$ ) and to both volume and surface heterogeneities in the alumina semi-transparent domain (2  $\mu\text{m}$ ).

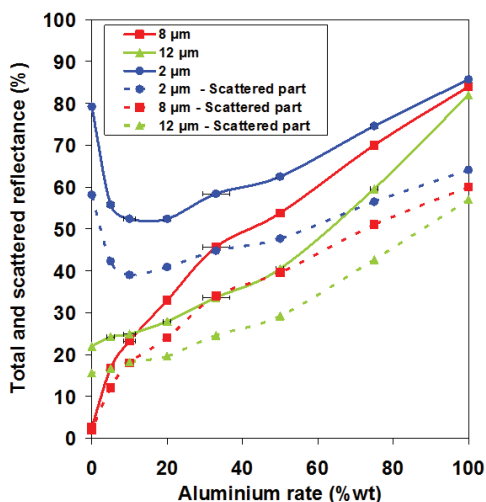


**Figure 4.5:** Total and scattered reflectance of the as-sprayed cermets depending on the wavelength as a function of Al rate.

### 3.3 Polished single material coatings

Cermets were polished to study the influence of the roughness on the optical response (Figure 4.7)

As-sprayed and polished alumina reflectance was identical except at 12  $\mu\text{m}$ . At 2  $\mu\text{m}$ , the reflectance of the polished specimen is still 80%, proving that the roughness has no influence at this wavelength unlike the volume heterogeneities. The scattering part is about 40%, because

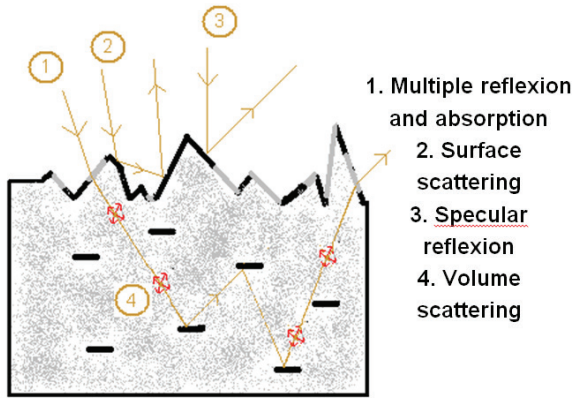


**Figure 4.6:** Schematic mechanisms occurring in the cermet in the transparent region.

pores scatter in the volume, as presumed. At  $8\ \mu\text{m}$ , alumina is almost fully absorbent. Indeed, it is characterised by none transparency and a weak reflectivity due to scattering. No roughness effect is revealed either. However, at  $12\ \mu\text{m}$ , the reflectivity of polished alumina increases. A part of the radiation which has been absorbed by the trapping of photons in surface heterogeneities is now reflected by specular reflection. For the aluminium coating, the polishing rises the reflectance because smaller quantity of photons can be absorbed by heterogeneities.

### 3.4 Polished cermet coatings

About the cermet, the argument has been conducted considering that the composition at the as-sprayed surface is the same that a slice in the volume. At  $2\ \mu\text{m}$ , the reflectance decreases up to an aluminium rate of 50%. That behaviour could be explained by the fact that a larger part of the radiation can penetrate in the material compared to the rough coatings. Indeed, the light would not be scattered by the surface roughness but absorbed as a result of multi reflexion on aluminium splats (Figure 4.6). For large amount of aluminium (upper than 50%), surface effects

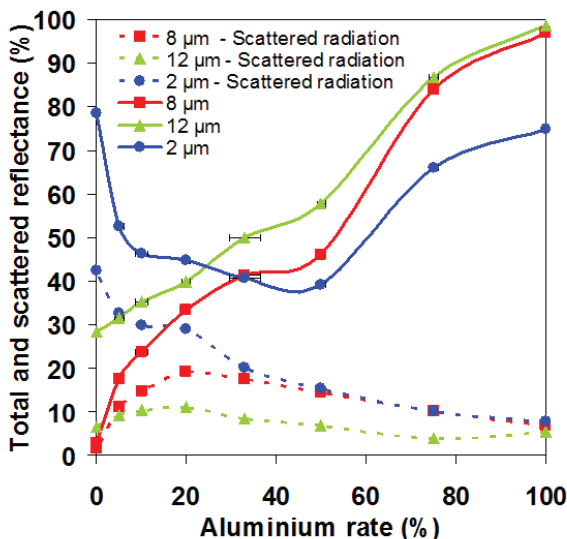


Figure 4.7: Total and scattered reflectance of the polished cermets depending on the wavelength as a function of Al rate.

are predominant, and so the reflectivity rises with aluminium content. At  $8\ \mu\text{m}$ , cermet reflectance does not significantly change with the aluminium rate, except for large amount of aluminium, meaning that polishing reduces the absorption part due to heterogeneities. Finally, the reflectance of a polished coating at  $12\ \mu\text{m}$  is higher than at  $8\ \mu\text{m}$ , proving that without polishing, surface scattering induces absorption.

### 3.5 Modeling considerations

The establishment of a model reproducing trends of the cermet reflectance is intended. In the opaque region, a rough calculation was realised. Knowing that photons can't penetrate in the volume, a possibility to predict the reflectance is therefore to assimilate the coating into a mosaic, with zones representing alumina and zones representing aluminium. The reflectance was estimated by taking into account the

experimental reflectivity of each pure polished material ( $R$ ), and their proportions on the surface, using a particle section (Figure 4.8). Then the following formula is used:  $R = p \times R(Al) + (1-p) \times R(Al_2O_3)$  With  $p$  the proportion of aluminium at the surface, calculated knowing the powder flow rate per second, and the surface of each particle. The spreading degree of alumina and aluminium lamellae was supposed to be equal. Calculated points are close to the experiment. However, Figure 4.8 shows the reflectance is a little underestimated at  $8 \mu\text{m}$  and not proportional to the aluminium amount. Indeed, the level of scattering light is higher for polished pure alumina and aluminium coatings than for the cermet. At  $12 \mu\text{m}$ , the two curves are very close because the scattering is almost constant, and so there is proportionality between the reflectance and the aluminium rate. Maxwell Garnett or Bruggeman methods are both not adapted because of the size range of lamellae. That means that the material should be more considered as a heterogeneous coating than a homogeneous one to model its optical response in the opaque region.

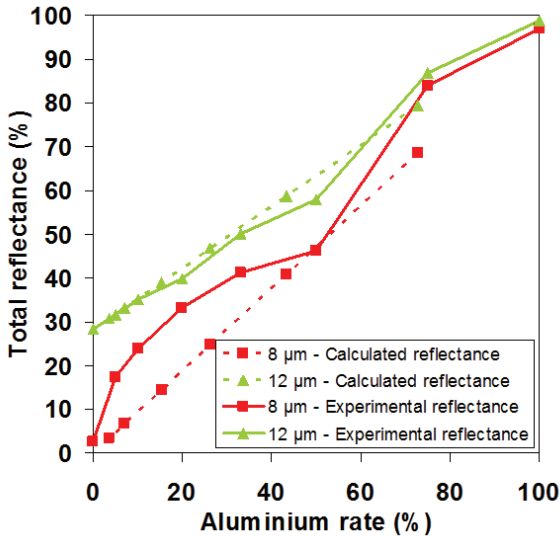


**Figure 4.8:** Experimental cermet reflectance and calculated reflectance depending on the wavelength as a function of Al rate.

## 4 Conclusion

Several  $\text{Al}_2\text{O}_3/\text{Al}$  cermets have been realised by APS, adjusting the aluminium rate to study the influence on the optical properties. Three characteristic wavelengths of specific domains of pure alumina were selected. In the transparent region, volume effects occur, and we notice that a cermet is less reflective than a pure alumina coating when the aluminium rate is low. Only surface effects occur in the opaque region, so the reflectance rises with the amount of aluminium. By changing plasma operating parameters, it will be worth investigating the impact of the total void content on the optical behaviour of plasma-sprayed cermets. Moreover, the next objective is to model the optical behaviour of plasma-sprayed cermets. A good approximation is to assimilate coatings into a mosaic of each material.

## References

1. P. Fauchais, "Understanding plasma spraying," *J. Phys. D: Applied Physics*, vol. 37, pp. R86–R108, 2004.
2. V. Debout, E. Bruneton, E. Meillot, S. Schelz, P. Abelard, P. Fauchais, and A. Vardelle, "Correlation between processing parameters, microstructure and optical properties for plasma-sprayed yttria-stabilized zirconia coatings." ISPC17, 2003.
3. M. Tului, F. Arezzo, and L. Pawlowski, "Optical properties of plasma sprayed semiconducting oxides," in *Proceeding of the International Thermal Spray Conference (ITSC)*, Düsseldorf, Germany., 2004.
4. V. Debout, A. Vardelle, P. Abelard, P. Fauchais, E. Bruneton, S. Schelz, and N. Branland, "Optical properties of yttria-stabilized zirconia plasma-sprayed coatings," in *Proceeding of the International Thermal Spray Conference (ITSC)*, 2006.
5. K. S. Caruso, D. G. Drewry, and J. S. Jones, "Heat treatment of plasma sprayed alumina: evolution of microstructure and optical properties," in *Advanced Ceramic Coatings and Interface II : Ceramic and Engineering Science Proceedings*, vol. 28, 2009, pp. 177–192.
6. G. Peelen, "Relation between microstructure and optical properties of polycrystalline alumina, science of ceramics," vol. 6, pp. pp.1–13, 1973.
7. O. Rozenbaum, D. S. Meneses, Y. D. Auger, S. Chermanne, and P. Echegut, "A spectroscopic method to measure the spectral emissivity of semi-transparent

materials up to high temperature," *Review of Sc. Instruments*, vol. 70, pp. 4020–4025, 1999.

8. J. Milo E. Whitson, "Handbook of the infrared optical properties of  $\text{Al}_2\text{O}_3$ , carbon,  $\text{MgO}$  and  $\text{ZrO}_2$ ," 1975.
9. M. Vardelle, "Etude de la structure des dépôts d'alumine obtenus par projection plasma en fonction des températures et des vitesses des particules au moment de leur impact sur la cible. in french," PhD thesis, 1980.